Photoacoustic radiation force on a microbubble

Hakan Erkol,* Esra Aytac-Kipergil, and Mehmet Burcin Unlu
Department of Physics, Bogazici University, Bebek, 34342 Istanbul, Turkey
(Received 21 April 2014; revised manuscript received 15 July 2014; published 5 August 2014)

We investigate the radiation force on a microbubble due to the photoacoustic wave which is generated by using a pulsed laser. In particular, we focus on the dependence of pulsed laser parameters on the radiation force. In order to do so, we first obtain a new and comprehensive analytical solution to the photoacoustic wave equation based on the Fourier transform for various absorption profiles. Then, we write an expression of the radiation force containing explicit laser parameters, pulse duration, and beamwidth of the laser. Furthermore, we calculate the primary radiation force acting on a microbubble. We show that laser parameters and the position of the microbubble relative to a photoacoustic source have a considerable effect on the primary radiation force. By means of recent developments in laser technologies that render tunability of pulse duration and repetition frequency possible, an adjustable radiation force can be applied to microbubbles. High spatial control of applied force is ensured on account of smaller focal spots achievable by focused optics. In this context, conventional piezoelectric acoustic source applications could be surpassed. In addition, it is possible to increase the radiation force by making source wavelength with the absorption peak of absorber concurrent. The application of photoacoustic radiation force can open a cache of opportunities such as manipulation of microbubbles used as contrast agents and as carrier vehicles for drugs and genes with a desired force along with *in vivo* applications.

DOI: 10.1103/PhysRevE.90.023001 PACS number(s): 47.10.−g, 78.20.Pa

I. INTRODUCTION

In recent years, photoacoustic imaging (PI) has evolved parallel to the drastic advances in lasers and ultrasonic transducers [1–14]. Photoacoustic imaging, which may be employed either as tomographic or microscopic imaging, uses absorption of the photon energy to produce contrast between absorbing and nonabsorbing media [15]. A short laser pulse is sent to an imaging sample, and thermal expansion occurs in the focal point of the laser. As a result of the thermal expansion, a pressure wave is generated and propagates through the medium to be received by ultrasonic transducers. Here pulse duration of the laser is required to be sufficiently short to ensure thermal confinement and stress confinement conditions [12].

Photoacoustic imaging has various applications from material characterization to biomedical sciences [16–21]. PI takes the advantage of high optical contrast and high ultrasonic resolution [22]. Besides, PI is safe for *in vivo* tissue imaging since it has a nonionizing absorption mechanism. Considering these particular advantages, PI is a promising technique for biomedical optics [23,24].

Resolution and contrast of PI depend primarily on laser parameters. Thus, developing a model that reveals the dependency of the photoacoustic signal on laser parameters will lead researchers to achieve optimal values for different applications.

Many authors have been working on the generation of photoacoustic signals. For example, Sigrist and Kneubühl [25] developed a model for Gaussian radial profiles; however, their model does not contain explicit pulse duration dependency. Lai and Young [26] presented a theory of the pulsed photoacoustic method for a weakly absorbing liquid. They studied the analytical and numerical results for laser beams with Gaussian shaped temporal and radial profiles using the far-field approximation. Their results are derived for cylindrical acoustic waves stimulated by a pulsed laser. In addition, Hoelen *et al.* [2] developed Sigrist and Kneubühl's models [25] and obtained pressure distribution depending on radius for a Gaussian spatiotemporal source formation. They used spherical, cylindrical, and planar absorption distributions. Their approach is to convolve the solution of photoacoustic wave equation for Dirac delta excitation with a pulsed signal of finite duration in time domain. For low frequencies, Diebold *et al.* [27] derived theorems in one, two, and three dimensions for short pulse excitation of fluid bodies and obtained the photoacoustic wave as a mapping of the spatial distribution of heat generated by the excitation. Moreover, Inkov *et al.* [28] studied the acoustic problem of thermo-optical sound excitation in an inhomogeneous medium for a one-dimensional case taking into consideration that the photoacoustic effect is in the linear regime. Applying boundary conditions, they solved the photoacoustic wave equation utilizing the integral of the distribution of heat sources of an absorbing particle in a liquid. Kozhushko *et al.* [29] presented a theory of the excitation of a photoacoustic transient by an object with a Gaussian distribution of photoacoustic sources approximating the temporal profile by the Dirac δ distribution. They also investigated a single array element response coming from an arbitrarily located point source experimentally. Diebold and Westervelt [30] examined the photoacoustic effect generated by a spherical droplet in a fluid. They obtained frequency domain and time domain pressure wave solutions to a boundary-value problem for a light pulse represented by the Dirac δ function. Calasso *et al.* [31] obtained the far-field d'Alembert solution to the photoacoustic wave equation for a nonlinear source term using Laplace transform. Wang [12,24] also studied the photoacoustic equation for Dirac δ point distributions of the spatiotemporal profiles. Anastasio *et al.* [32] studied the photoacoustic tomography image reconstruction problem using the Fourier transform and time-harmonic inverse source concepts. They obtained a mathematical expression giving a relation between the photoacoustic pressure wave-field data and the three-dimensional

*hakan.erkol@boun.edu.tr

Fourier transform of the optical absorption distribution. They also derived exact and approximate analytic reconstruction formulas.

It is well known that acoustic waves apply primary and secondary forces on acoustic absorbers due to the exchange of momentum. These forces have been investigated in the literature extensively. An important example is the acoustic forces on a microbubble [33–39]. These forces affect the motion of the microbubbles considerably. The microbubbles treated as compressible spheres are used as contrast agents to increase the intensity of scattered echoes from blood. The microbubble is mainly composed of gas enclosed by albumin [34].

Leighton [33] and Dayton *et al.* [34] studied the effect of the primary and the secondary radiation force on microbubbles both theoretically and experimentally. They showed that the displacement due to the primary force is linearly dependent on the pulse repetition frequency and nonlinearly dependent on the acoustic pressure wave.

Applying the primary radiation force, the flow of microbubbles can be manipulated to improve image quality and drug delivery. Microbubbles are selected through the vasculature of tumor because of their micron size, enhancement of cell membrane, and vascular permeability by insonated microbubbles is also presented. Because of those properties, they have been proposed as carrier vehicles for drugs and genes [40,41]. Thus, manipulation of microbubbles to the location of interest in the body is of paramount significance. Jones and Stride showed experimentally that ultrasound contrast agent microbubbles can be trapped in three dimensions using optical tweezers to confine the microbubble. They also measured the maximum transverse drag force that is necessary to trap the microbubble before it escapes [42].

Besides primary or secondary forces, the manipulation or encapsulation of cells can be achieved by utilizing photoacoustic tweezers. Zharov *et al.* [43] presented a nonionizing optical technique to control particles by using a pulsed laser. Due to the photoacoustic pressure wave created in an absorbing medium, the manipulation of the particle around the medium can be provided. They presented a force expression introducing the action of the acoustic field with time-averaged kinetic and potential energy densities in the acoustic wave. They also validated their results by conducting experiments.

It is important to note that in the above literature, acoustic radiation force is generated by an ultrasound transducer. Usually a pulser-receiver is used to generate the acoustic wave in the range of 1 to 10 kHz. Therefore, the tunability of the force is limited by the frequency of the transducer and the repetition rate of the ultrasound source.

In contrast, the acoustic wave generated by a pulsed laser offers a much wider range of tunability of the radiation force. Adjusting the laser parameters such as beamwidth, pulse duration, and repetition rate enables a controllable force that can be used to manipulate micron-sized acoustic absorbers.

We establish an explicit link between the pulsed laser parameters and the photoacoustic radiation force. In order to accomplish this, we first solve the photoacoustic wave equation analytically without the far-field approximation. This solution leads to a pressure wave from which the photoacoustic radiation force can be calculated.

It is important to note that in the literature previously, the photoacoustic wave equation had been mostly solved for the Dirac δ-shaped or Gaussian profiles. Even though a couple of works dealt with the photoacoustic equation for both Gaussian radial and temporal profiles, their solutions were based on some approximations (such as the far-field approximation) or for some boundary conditions.

The difference in this manuscript is twofold. The first difference comes from the solution of the photoacoustic wave equation without the far-field approximation. Our method is different from the previous works in the sense that we also use a Gaussian radial absorption profile which reveals the effect of the laser parameters on the photoacoustic signal. Combining this expression with the acoustic radiation force equation [33,34] for a microbubble, we calculate the photoacoustic radiation force for various laser parameters (pulse duration, beamwidth, and pulse repetition frequency). This enables the investigation of the variation of the force with respect to the corresponding parameters. Our method is viable if the resonant frequency of the bubble and the center frequency of the wave are very close to each other. Another important limitation is that the acoustic radiation force presented by Leighton [33] and Dayton *et al.* [34] is derived for the narrowband acoustic excitation. Although the photoacoustic wave is usually broadband, if the pulse duration is sufficiently long, then the wave is narrowband [44]. The calculated force turns out to be in the range of piconewtons and nanonewtons due to the facts that (i) the absorption spectrum of a chromophore varies for different wavelengths and (ii) laser parameters can be adjusted. At least forces of a few hundred piconewtons are required to manipulate the microbubbles in biological applications [45]. In addition, viscoelastic properties of the microbubbles can be measured applying considerably small forces ($<$10 pN) [46]. In contradistinction for optical tweezers, acoustic tweezers, and piezoelectric acoustic sources, photoacoustic technique may apply acoustic radiation force with high spatial control on contrast agents. Hence, photoacoustic source outperforms conventional piezoelectric acoustic source in which high spatial control of applied force is ensured due to smaller focal spots achievable by focused optics.

II. THEORY AND METHOD

The photoacoustic wave resulted from light absorption obeys the following wave equation:

$$\left(\nabla^2 - \frac{1}{v_s^2}\frac{\partial^2}{\partial t^2}\right) p(\mathbf{r},t) = -\frac{\beta}{\kappa v_s^2}\frac{\partial^2 T(\mathbf{r},t)}{\partial t^2}. \quad (1)$$

The left hand side of Eq. (1) represents the wave propagation where v_s is the speed of sound, and $p(\mathbf{r},t)$ is the photoacoustic wave at position $\mathbf{r}$ and time t. The right hand side of Eq. (1) describes the photoacoustic source where β is the thermal coefficient of volume expansion, κ is the isothermal compressibility, and $T(\mathbf{r},t)$ is the increase in temperature at position $\mathbf{r}$ and time t [12].

In photoacoustics, the laser pulse duration is less than the acoustic confinement time. The confinement time is also less than the thermal confinement time. For this reason, the laser pulse is short. Hence, for a short laser pulse, the thermal

equation becomes

$$\rho C_V \frac{\partial T(\mathbf{r},t)}{\partial t} = H(\mathbf{r},t), \tag{2}$$

where H is the heating function, the amount of heat generated by light absorption per unit volume and per unit time, and ρ and C_V denote density and the specific heat capacity at constant volume, respectively [12,24]. In photoacoustics, since absorption is dominant, H can be treated as the optical absorption coefficient μ_a times the light fluence rate F ($H = \mu_a F$).

Thus, for a short laser pulse, the photoacoustic wave holds for the equation

$$\left(\nabla^2 - \frac{1}{v_s^2}\frac{\partial^2}{\partial t^2}\right) p(\mathbf{r},t) = -\frac{\beta}{C_P}\frac{\partial H(\mathbf{r},t)}{\partial t}, \tag{3}$$

where r is the radial coordinate and C_P is the specific heat capacity at constant pressure, respectively.

The solutions for the photoacoustic wave equation can be obtained by using the Green's function approach [12,47]. Wang solved the photoacoustic equation in the time domain by treating the source term as a combination of spatial and temporal profiles approximated by Dirac δ point distributions [12,24]. In this work, for a Gaussian temporal profile, we first consider the radial part of the source term of the photoacoustic equation as rectangular and solve the equation in frequency domain. Hence, using the inverse Fourier transform, we obtain the solution for the equation in time domain.

We denote the source term of the photoacoustic wave equation (1) by $S(\mathbf{r},t)$,

$$S(\mathbf{r},t) \equiv -\frac{\beta}{C_P}\frac{\partial H(\mathbf{r},t)}{\partial t}. \tag{4}$$

Here the temporal and the radial parts of the source term can be decomposed as

$$H(\mathbf{r},t) = A(\mathbf{r})H(t). \tag{5}$$

For a Gaussian temporal profile, the heating function is expressed by

$$H(t) = \frac{\exp\left(-\frac{t^2}{2\tau^2}\right)}{\sqrt{2\pi\tau^2}}, \tag{6}$$

where τ is the standard deviation or the pulse duration of the laser. For a stress confinement case where laser pulse width is much shorter than the stress relaxation time, the initial pressure rise just after the pulse, $p_0(\mathbf{r})$, can be written as [12,24]

$$p_0(\mathbf{r}) = \frac{\beta T(\mathbf{r})}{\kappa}. \tag{7}$$

If all the absorbed electromagnetic energy is converted into heat and nonthermal relaxation is neglected, then the increase in temperature resulted from the laser pulse can be written as

$$T(\mathbf{r}) = \frac{A(\mathbf{r})}{\rho C_V}. \tag{8}$$

Combining Eq. (7) with Eq. (8) and writing

$$\kappa = \frac{C_P}{\rho v_s^2 C_V}, \tag{9}$$

we get

$$A(\mathbf{r}) = \frac{p_0(\mathbf{r})}{v_s^2}\frac{C_P}{\beta}. \tag{10}$$

Substituting Eq. (10) into Eq. (5) leads to

$$S(\mathbf{r},t) = -\frac{p_0(\mathbf{r})}{v_s^2}\frac{\partial}{\partial t}\left[\frac{\exp\left(-\frac{t^2}{2\tau^2}\right)}{\sqrt{2\pi\tau^2}}\right] \tag{11}$$

$$= \frac{1}{\sqrt{2\pi}\tau^3}\frac{p_0(\mathbf{r})}{v_s^2} t \exp\left(-\frac{t^2}{2\tau^2}\right). \tag{12}$$

Fourier transform of $S(\mathbf{r},t)$ yields

$$\tilde{S}(\mathbf{r},\omega) = \frac{1}{\sqrt{2\pi}\tau^3}\frac{p_0(\mathbf{r})}{v_s^2}\int_{-\infty}^{\infty} t \exp\left(-\frac{t^2}{2\tau^2}\right)\exp(i\omega t)dt \tag{13}$$

$$= \frac{i}{\sqrt{2\pi}}\frac{p_0(\mathbf{r})}{v_s^2}\omega \exp\left(-\frac{\tau^2\omega^2}{2}\right). \tag{14}$$

Using Fourier convention, $p(\mathbf{r},t) = \frac{1}{\sqrt{2\pi}}\int_{-\infty}^{\infty}\tilde{p}(\mathbf{r},\omega)\exp(-i\omega t)d\omega$, the photoacoustic wave equation (1) can be expressed in frequency domain

$$\nabla^2\tilde{p}(\mathbf{r},\omega) + \frac{\omega^2}{v_s^2}\tilde{p}(\mathbf{r},\omega) = i\frac{p_0(\mathbf{r})}{v_s^2}\omega\exp\left(-\frac{\tau^2\omega^2}{2}\right). \tag{15}$$

The Green's function of Eq. (15) is given by the expression [47]

$$\tilde{G}(\mathbf{r},\mathbf{r}';\omega) = -\frac{1}{4\pi|\mathbf{r}-\mathbf{r}'|}\exp\left(i\frac{\omega}{v_s}|\mathbf{r}-\mathbf{r}'|\right), \tag{16}$$

where the Green's function is an outgoing spherical wave for $|\mathbf{r}-\mathbf{r}'| \to \infty$.

The solution in the ω domain can be found by evaluating the following integral:

$$\tilde{p}(\mathbf{r},\omega) = \int \tilde{G}(\mathbf{r},\mathbf{r}';\omega)\tilde{S}(\mathbf{r}';\omega)d^3r'. \tag{17}$$

Substituting Eqs. (14) and (16) into Eq. (17) gives

$$\tilde{p}(\mathbf{r},\omega) = -\frac{i}{4\pi}\frac{\omega}{v_s^2}\exp\left(-\frac{\tau^2\omega^2}{2}\right) \times \int p_0(r')\frac{\exp\left(i\frac{\omega}{v_s}|\mathbf{r}-\mathbf{r}'|\right)}{|\mathbf{r}-\mathbf{r}'|}d^3r'. \tag{18}$$

When a spherical object of radius R is excited by a short pulsed laser beam, the initial pressure p_0 is created inside the object so that the initial pressure distribution can be written as [12,24]

$$p_0(r) = p_0\theta(r)\theta(-r+R), \tag{19}$$

where θ is the Heaviside step function.

Writing Eq. (19) into Eq. (18) and taking $\mathbf{r}$ along the z axis, we get

$$\tilde{p}(r,\omega) = -\frac{ip_0}{4\pi}\frac{\omega}{v_s^2}\exp\left(-\frac{\tau^2\omega^2}{2}\right) \times \int_0^{2\pi}d\phi'\int_0^R (r')^2dr'\int_{-1}^{1}\frac{\exp\left(i\frac{\omega}{v_s}|\mathbf{r}-\mathbf{r}'|\right)}{|\mathbf{r}-\mathbf{r}'|}d\mu', \tag{20}$$

where $\mu' = \cos\theta'$ and $|\mathbf{r} - \mathbf{r}'| = \sqrt{r^2 + r'^2 - 2rr'\mu'}$. Inserting the result of the integral

$$\int_{-1}^{1} \frac{\exp\left[i\frac{\omega}{v_s}(r^2 + r'^2 - 2rr'\mu')^{1/2}\right]}{(r^2 + r'^2 - 2rr'\mu')^{1/2}} d\mu' = -\frac{1}{irr'\frac{\omega}{v_s}}\left\{\exp\left[i\frac{\omega}{v_s}(r - r')\right] - \exp\left[i\frac{\omega}{v_s}(r + r')\right]\right\} \tag{21}$$

into Eq. (20) gives the solution in the ω domain

$$\tilde{p}(r,\omega) = ip_0\frac{v_s}{r}\frac{\exp\left(-\frac{\tau^2\omega^2}{2} + i\frac{\omega}{v_s}r\right)}{\omega^2} \times \left[\frac{\omega}{v_s}R\cos\left(\frac{\omega}{v_s}R\right) - \sin\left(\frac{\omega}{v_s}R\right)\right], \tag{22}$$

where $r > R$ or $r > r'$.

An inverse Fourier transform of $\tilde{p}(r,\omega)$ leads to

$$p(r,t) = \frac{i}{\sqrt{2\pi}}p_0\frac{v_s}{r}\int_{-\infty}^{\infty}\frac{\exp\left(-\frac{\tau^2\omega^2}{2} + i\frac{\omega}{v_s}r - i\omega t\right)}{\omega^2} \times \left[\frac{\omega}{v_s}R\cos\left(\frac{\omega}{v_s}R\right) - \sin\left(\frac{\omega}{v_s}R\right)\right]d\omega. \tag{23}$$

Writing $\cos(\frac{\omega}{v_s}R)$ and $\sin(\frac{\omega}{v_s}R)$ in terms of exponentials into Eq. (23) yields

$$p(r,t) = \frac{ip_0}{2\sqrt{2\pi}}\frac{R}{r}\int_{-\infty}^{\infty}\left\{\frac{\exp\left[-\frac{\tau^2\omega^2}{2} + i\omega\left(\frac{r+R}{v_s} - t\right)\right]}{\omega} + \frac{\exp\left[-\frac{\tau^2\omega^2}{2} + i\omega\left(\frac{r-R}{v_s} - t\right)\right]}{\omega}\right\}d\omega + \frac{1}{2\sqrt{2\pi}}p_0\frac{v_s}{r} \times \int_{-\infty}^{\infty}\left\{\frac{\exp\left[-\frac{\tau^2\omega^2}{2} + i\omega\left(\frac{r+R}{v_s} - t\right)\right]}{\omega^2} - \frac{\exp\left[-\frac{\tau^2\omega^2}{2} + i\omega\left(\frac{r-R}{v_s} - t\right)\right]}{\omega^2}\right\}d\omega. \tag{24}$$

If the following I_1 and I_2 integrals are solved, then the solution of the photoacoustic equation can be obtained,

$$I_1 = \int_{-\infty}^{\infty}\frac{\exp\left[-\frac{\tau^2\omega^2}{2} + i\omega(\frac{r+R}{v_s} - t)\right]}{\omega}d\omega, \tag{25}$$

$$I_2 = \int_{-\infty}^{\infty}\frac{\exp\left[-\frac{\tau^2\omega^2}{2} + i\omega(\frac{r+R}{v_s} - t)\right]}{\omega^2}d\omega. \tag{26}$$

These I_1 and I_2 kinds of integrals can be calculated carrying out the residue theorem [47].

To calculate an integral of the type

$$I = \int_{-\infty}^{\infty} f(z)\exp(i\alpha z)dz, \tag{27}$$

the Jordan lemma has to be satisfied. The Jordan lemma states that if $f(z) \to 0$ as $z \to \infty$, then

$$\lim_{R\to\infty}\int_{C_R} f(z)\exp(i\alpha z)dz = 0, \tag{28}$$

where C_R is a circular path of infinite radius on the upper z plane for $\alpha > 0$. The I_1 integral in complex z plane can be written as

$$\oint\frac{\exp\left[-\frac{\tau^2z^2}{2} + iz\left(\frac{r+R}{v_s} - t\right)\right]}{z}dz = \int_{-\infty}^{\infty}\frac{\exp\left[-\frac{\tau^2x^2}{2} + ix\left(\frac{r+R}{v_s} - t\right)\right]}{x}dx + \lim_{R\to\infty}\int_{C_R}\frac{\exp\left[-\frac{\tau^2z^2}{2} + iz\left(\frac{r+R}{v_s} - t\right)\right]}{z}dz. \tag{29}$$

Here if $(\frac{r+R}{v_s} - t) > 0$, the second integral on the right hand side of Eq. (29) becomes zero due to the Jordan lemma.

Applying the residue theorem at $z = 0$ gives

$$\oint\frac{\exp\left[-\frac{\tau^2z^2}{2} + iz\left(\frac{r+R}{v_s} - t\right)\right]}{z}dz = \begin{cases}\pi i\lim_{z\to 0} z\frac{\exp[-\frac{\tau^2z^2}{2} + iz(\frac{r+R}{v_s} - t)]}{z} & \text{if } (\frac{r+R}{v_s} - t) > 0,\\ -\pi i\lim_{z\to 0} z\frac{\exp[-\frac{\tau^2z^2}{2} + iz(\frac{r+R}{v_s} - t)]}{z} & \text{if } (\frac{r+R}{v_s} - t) < 0.\end{cases} \tag{30}$$

Hence,

$$I_1 = \pi i\,\mathrm{sgn}\left(\frac{r+R}{v_s} - t\right) \tag{31}$$

where $\mathrm{sgn}(x)$ is the signum function. Following the similar steps and taking into consideration that $z = 0$ is a second order pole, I_2 can be found as

$$I_2 = -\pi\left(\frac{r+R}{v_s} - t\right)\mathrm{sgn}\left(\frac{r+R}{v_s} - t\right). \tag{32}$$

Substituting Eqs. (31) and (32) into Eq. (24) leads to the following solution of the photoacoustic equation in time domain for a spherical object heated homogeneously by a short laser pulse having a Gaussian temporal profile

$$p(r,t) = \frac{1}{2}\sqrt{\frac{\pi}{2}}\frac{p_0}{r}\left[(r - v_st)\,\mathrm{sgn}\left(\frac{r+R}{v_s} - t\right) + (-r + v_st)\,\mathrm{sgn}\left(\frac{r-R}{v_s} - t\right)\right]. \tag{33}$$

Diebold *et al.* [27,30] derived expressions in an original way for the photoacoustic response from a uniformly irradiated sphere. They used a δ function heating pulse and amplitude modulated radiation. Different from their work, in our study, the temporal part of the source term is taken as Gaussian and our solution is based on the complex integration technique. As can be seen in the next section, the Gaussian temporal part reveals the effect of laser parameters on the photoacoustic wave in an overt manner. In this way, regarding the application, parameters can be adjusted to utilize the photoacoustic wave and the required primary radiation force.

If a pulsed laser is sent to a spherical object of radius R, the object is heated and an initial pressure p_0 is created inside the object. There are three cases based on the propagation time when observation point is outside the spherical object [24,48].

(i) If $r - R > v_s t$, the spherical object does not intersect with the spherical shell of radius $v_s t$ which is centered at the observation point so that $p(r,t)$ becomes zero.

(ii) If $v_s t$ is between the interval $[r - R, r + R]$, the heated spherical object touches the spherical shell of radius $v_s t$. Therefore, the pressure can be described by Eq. (33).

(iii) If $r + R < v_s t$, then the spherical object cannot intersect with the spherical shell; thus, $p(r,t)$ becomes zero.

Therefore, these three cases can be combined into an equation by utilizing the Heaviside step function, $\theta(x)$,

$$p(r,t) = \frac{1}{2}\sqrt{\frac{\pi}{2}}\frac{p_0}{r}\left\{(r - v_s t)\,\mathrm{sgn}\left(\frac{r+R}{v_s} - t\right) + (-r + v_s t)\;\mathrm{sgn}\left(\frac{r-R}{v_s} - t\right)\right\} \times \theta(r - |R - v_s t|)\theta(-r + R + v_s t), \tag{34}$$

for outside the object ($r > R$).

Moreover, if the pulse duration is sufficiently long and the radial distance r is greater than the radius of the absorber, $\frac{r}{R} \gg 1$, our method yields the far-field based solution, which was presented by Diebold *et al.* [49]. For any slow heat deposition from an incompressible spherical particle, Diebold *et al.* [49] obtained a photoacoustic wave,

$$p(r,t) = \frac{\beta a}{8\pi^2 \hat{r} C_P}\frac{d}{dt}q\left(t - \frac{r}{c}\right), \tag{35}$$

where a is the radius, $\hat{r} = \frac{r}{a}$, and q is the heat flux vector.

In our case, for the far-field approximation $\frac{r'}{r} \ll 1$,

$$\frac{\exp\left(i\frac{\omega}{v_s}|\mathbf{r} - \mathbf{r}'|\right)}{|\mathbf{r} - \mathbf{r}'|} \approx \frac{\exp\left(i\frac{\omega}{v_s}r\right)}{r} + \frac{\exp\left(i\frac{\omega}{v_s}r\right)}{r}\left(1 - i\frac{\omega}{v_s}r\right)\mu'\frac{r'}{r}, \tag{36}$$

where $\mu' = \cos\theta'$. Substituting Eq. (36) into Eq. (20) and using the inverse Fourier transform gives the normalized solution

$$\tilde{p}(r,t) \sim -\frac{R^3}{v_s^3\tau^3}\left(-1 + \frac{v_s t}{r}\right)\exp\left[-\frac{(r - v_s t)^2}{2v_s^2\tau^2}\right]. \tag{37}$$

Note that for $R \ll 1$, the same solution can also be obtained expanding cosine and sine terms in series in Eq. (22), $\cos(\frac{\omega}{v_s}R) \approx 1 - \frac{(\frac{\omega}{v_s}R)^2}{2}$ and $\sin(\frac{\omega}{v_s}R) \approx \frac{\omega}{v_s}R - \frac{(\frac{\omega}{v_s}R)^3}{6}$.

Now we want to obtain an expression using Diebold's result given by Eq. (35). Multiplying the heat flux from the absorber by the number of the absorbers per unit volume yields the heat flux in terms of the heating function [50],

$$q(r,t) = c\,\frac{p_0 C_P R}{v_s^2\beta}\frac{\exp\left(-\frac{t^2}{2\tau^2}\right)}{\sqrt{2\pi}\,\tau^2}, \tag{38}$$

where c is a dimensionless quantity related to the ratio of the volume of domain and the volume of the absorber. Substituting Eq. (38) into Eq. (35) leads to the same normalized solution obtained by Eq. (37) except for the normalization constants. If the pulse duration is long enough, $\frac{v_s\tau}{R} \approx 1$, Eq. (37) can be written as

$$\tilde{p}(r,t) \sim \left(1 - \frac{v_s t}{r}\right)\exp\left[-\frac{\left(\frac{v_s t}{R} - \frac{r}{R}\right)^2}{2}\right]. \tag{39}$$

The pressure rise just after the laser excitation can be expressed in terms of the optical absorption coefficient and the optical fluence considering a fractional volume expansion,

$$\frac{dV}{V} = -\kappa p + \beta T, \tag{40}$$

where T is the increase in temperature. For a very short laser pulse which is in the thermal and the stress confinements, the change of the volume can be neglected so that the increase in pressure just after the excitation can be expressed by

$$p_0 = \frac{\beta T}{\kappa}. \tag{41}$$

Substituting $T = \eta_{\mathrm{th}}\frac{A}{\rho C_V}$ into Eq. (41) leads to

$$p_0 = \frac{\beta}{\kappa\rho C_V}\eta_{\mathrm{th}}A, \tag{42}$$

where η_{th} is the fraction of the laser energy converted into heat. Defining Grueneisen parameter $\Gamma = \frac{\beta}{\kappa\rho C_V}$ and writing $A = \mu_a F$, Eq. (42) becomes

$$p_0 = \Gamma\eta_{\mathrm{th}}\mu_a F, \tag{43}$$

where μ_a and F stand for the optical absorption coefficient and the optical fluence, respectively.

The photoacoustic signals can be detected if an ultrasonic transducer is located outside the spherical object. Thus, the optical absorption coefficient μ_a can be calculated by inserting the detected signal and the other parameters in Eq. (34).

A. Solution of photoacoustic wave equation for a Gaussian radial absorption profile

In this section, we treat the radial absorption profile as Gaussian, which is a more comprehensive case compared to the uniform radial profile case,

$$p_0(r) = p_0\exp\left(-\frac{r^2}{2\sigma^2}\right)\theta(r)\theta(-r + R), \tag{44}$$

where σ is the standard deviation or beamwidth of the laser. Fourier transform of $p(r,t)$ gives

$$\tilde{p}(r,\omega) = \frac{p_0}{2\pi}\frac{1}{v_s r}\exp\left[-\frac{\tau^2\omega^2}{2}\right]\left(\int_0^R r'\exp\left(-\frac{r'^2}{2\sigma^2}\right) \times \left\{\exp\left[i\frac{\omega}{v_s}(r - r')\right] - \exp\left[i\frac{\omega}{v_s}(r + r')\right]\right\}dr'\right). \tag{45}$$

The solution of the photoacoustic equation in time domain can be obtained by calculating the following integral:

$$p(r,t) = \frac{p_0}{2\sqrt{2\pi}}\frac{1}{v_s r}\int_0^R r'\exp\left(-\frac{r'^2}{2\sigma^2}\right) \times \int_{-\infty}^{\infty}\left\{\exp\left[-\frac{\tau^2\omega^2}{2} + i\omega\left(\frac{r - r'}{v_s} - t\right)\right] - \exp\left[-\frac{\tau^2\omega^2}{2} + i\omega\left(\frac{r + r'}{v_s} - t\right)\right]\right\}d\omega dr'. \tag{46}$$

Substituting

$$\int_{-\infty}^{\infty} \exp\left[-\frac{\tau^2\omega^2}{2} + i\omega\left(\frac{r \mp r'}{v_s} - t\right)\right] d\omega = \frac{\sqrt{2\pi}}{\tau} \exp\left[-\frac{\left(\frac{r\mp r'}{v_s} - t\right)^2}{2\sigma^2}\right] \tag{47}$$

into Eq. (46) leads to

$$p(r,t) = \frac{p_0}{2}\frac{1}{v_s r\sigma}\int_0^R r' \left\{\exp\left[-\frac{r'^2}{2\sigma^2} - \frac{\left(\frac{r-r'}{v_s} - t\right)^2}{2\sigma^2}\right] - \exp\left[-\frac{r'^2}{2\sigma^2} - \frac{\left(\frac{r+r'}{v_s} - t\right)^2}{2\sigma^2}\right]\right\} dr' \tag{48}$$

for outside the object ($r > R$). Calculations of

$$J_{1,2} = \int_0^R r' \exp\left[-\frac{r'^2}{2\sigma^2} - \frac{\left(\frac{r\mp r'}{v_s} - t\right)^2}{2\sigma^2}\right] dr' \tag{49}$$

integrals, which are on the right hand side of Eq. (48), yield

$$J_1 = \int_0^R r' \exp\left[-\frac{r'^2}{2\sigma^2} - \frac{(\frac{r-r'}{v_s} - t)^2}{2\tau^2}\right] dr' \tag{50}$$

$$\begin{aligned} &= \frac{\tau\sigma^2 v_s}{2\left(\sigma^2 + \tau^2 v_s^2\right)^{3/2}} \exp\left[-\frac{(r - v_s t)^2}{2\tau^2 v_s^2}\right]\left(\sqrt{2\pi}\sigma(r - v_s t)\exp\left[\frac{\sigma^2(r - v_s t)^2}{2\tau^2 v_s^2\left(\sigma^2 + \tau^2 v_s^2\right)}\right]\right. \\ &\quad \times\left\{\operatorname{erf}\left[\frac{\sigma^2(-r + R + v_s t) + R\tau^2 v_s^2}{\sqrt{2}\tau\sigma v_s\sqrt{\sigma^2 + \tau^2 v_s^2}}\right] + \operatorname{erf}\left[\frac{\sigma(r - v_s t)}{\sqrt{2}\tau v_s\sqrt{\sigma^2 + \tau^2 v_s^2}}\right]\right\} \\ &\quad \left. - 2\tau v_s\sqrt{\sigma^2 + \tau^2 v_s^2}\left\{\exp\left[\frac{1}{2}R\left(-\frac{-2r + R + 2v_s t}{\tau^2 v_s^2} - \frac{R}{\sigma^2}\right)\right] - 1\right\}\right) \end{aligned} \tag{51}$$

and

$$J_2 = \int_0^R r' \exp\left[-\frac{r'^2}{2\sigma^2} - \frac{\left(\frac{r+r'}{v_s} - t\right)^2}{2\tau^2}\right] dr' \tag{52}$$

$$\begin{aligned} &= \frac{\tau\sigma^2 v_s}{2\left(\sigma^2 + \tau^2 v_s^2\right)^{3/2}} \exp\left[-\frac{(r + R - v_s t)^2}{2\tau^2 v_s^2} - \frac{R^2}{2\sigma^2}\right]\left(\sqrt{2\pi}\sigma(r - v_s t)\exp\left\{\frac{\left[\sigma^2(r + R - v_s t) + R\tau^2 v_s^2\right]^2}{2\tau^2\sigma^2 v_s^2\left(\sigma^2 + \tau^2 v_s^2\right)}\right\}\right. \\ &\quad \times\left\{\operatorname{erf}\left[\frac{\sigma(r - v_s t)}{\sqrt{2}\tau v_s\sqrt{\sigma^2 + \tau^2 v_s^2}}\right] - \operatorname{erf}\left[\frac{\sigma^2(r + R - v_s t) + R\tau^2 v_s^2}{\sqrt{2}\tau\sigma v_s\sqrt{\sigma^2 + \tau^2 v_s^2}}\right]\right\} \\ &\quad \left. + 2\tau v_s\sqrt{\sigma^2 + \tau^2 v_s^2}\left(\exp\left\{\frac{R[2(r - v_s t) + \frac{R\tau^2 v_s^2}{\sigma^2} + R]}{2\tau^2 v_s^2}\right\} - 1\right)\right), \end{aligned} \tag{53}$$

respectively, where $\operatorname{erf}(x)$ is the error function.

Therefore, substituting the integrals J_1 and J_2 into Eq. (48) and considering the three cases based on the propagation time mentioned in the previous section gives

$$\begin{aligned} p(r,t) &= \frac{p_0\sigma^2}{4r\left(\sigma^2 + \tau^2 v_s^2\right)^{3/2}} \exp\left[-\frac{2R(r - v_s t) + 2(r - v_s t)^2 + R^2}{2\tau^2 v_s^2} - \frac{R^2}{2\sigma^2}\right] \\ &\quad \times\left(\sqrt{2\pi}\sigma(r - v_s t)\left\{\operatorname{erf}\left[\frac{\sigma^2(-r + R + v_s t) + R\tau^2 v_s^2}{\sqrt{2}\tau\sigma v_s\sqrt{\sigma^2 + \tau^2 v_s^2}}\right]\exp\left[\frac{(r + R - v_s t)^2}{2\tau^2 v_s^2} + \frac{\sigma^2(r - v_s t)^2}{2\tau^2 v_s^2\left(\sigma^2 + \tau^2 v_s^2\right)} + \frac{R^2}{2\sigma^2}\right]\right.\right. \\ &\quad \left.\left. + \operatorname{erf}\left[\frac{\sigma^2(r + R - v_s t) + R\tau^2 v_s^2}{\sqrt{2}\tau\sigma v_s\sqrt{\sigma^2 + \tau^2 v_s^2}}\right]\exp\left\{\frac{\frac{[\sigma^2(r+R-v_s t)+R\tau^2 v_s^2]^2}{\sigma^2(\sigma^2+\tau^2 v_s^2)} + (r - v_s t)^2}{2\tau^2 v_s^2}\right\}\right\}\right. \\ &\quad \left. - 2\tau v_s\sqrt{\sigma^2 + \tau^2 v_s^2}\exp\left[\frac{(r - v_s t)^2}{2\tau^2 v_s^2}\right]\left\{\exp\left[\frac{2R(r - v_s t)}{\tau^2 v_s^2}\right] - 1\right\}\right)\theta(r - |R - v_s t|)\theta(-r + R + v_s t) \end{aligned} \tag{54}$$

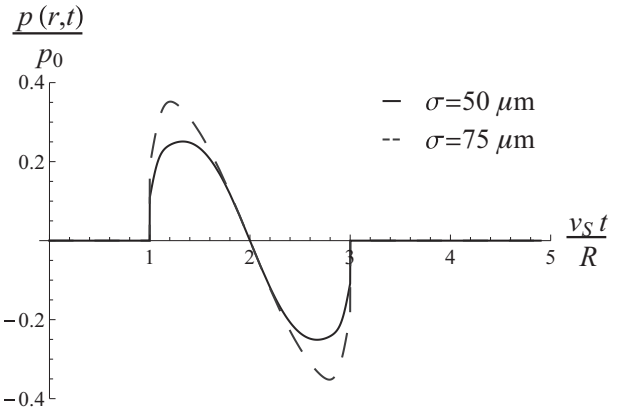

FIG. 1. Normalized photoacoustic wave $\frac{p(r,t)}{p_0}$ vs normalized time $\frac{v_s t}{R}$ at $r = 2R$ for the beamwidth (a) $\sigma = 50$ μm and (b) $\sigma = 75$ μm, where $R = 75$ μm and the pulse duration $\tau = 5$ ns.

for outside the spherical object. In order to relate the spherical object's parameters to the signal, $p_0 = \Gamma \eta_{\text{th}} \mu_a F$ can be written into Eq. (54).

Hence, Eq. (54) gives the photoacoustic wave generated by a short laser pulse which has both Gaussian temporal and radial profiles.

For biomedical applications, we take the values of the speed of the wave, the pulse duration of the laser, and the radius of the absorber, $v_s = 1480$ m/s, $\tau = 5$ ns, and $R = 75$ μm, respectively [12,51,52]. From Eq. (54), the behavior of a normalized photoacoustic wave with respect to the normalized time is obtained. Figure 1 shows the change of the normalized photoacoustic wave $\frac{p(r,t)}{p_0}$ as a function the normalized time $\frac{v_s t}{R}$ for the beamwidth of laser $\sigma = 50$ and 75 μm values. Figure 2 shows the change of the normalized amplitude of photoacoustic wave with increasing pulse duration τ for $\sigma = 25$, 50, and 75 μm.

III. EFFECT OF THE LASER PARAMETERS ON THE PRIMARY RADIATION FORCE ACTING ON A MICROBUBBLE

Leighton [33], Dayton *et al.* [34], Zheng and Apfel [35], Lee and Wang [36], Lofstedt and Putterman [37], Wu and Du [38],

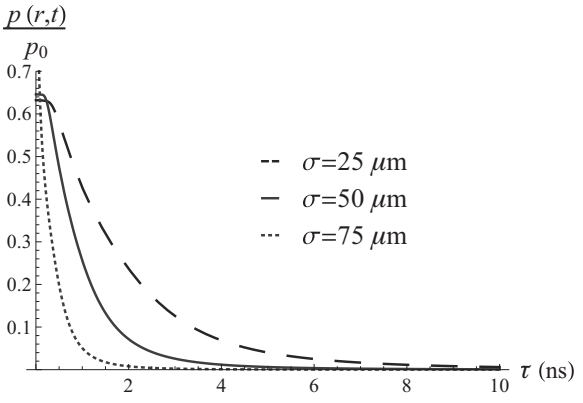

FIG. 2. Normalized amplitude of photoacoustic wave $\frac{p(r,t)}{p_0}$ vs pulse duration τ for the beamwidth $\sigma = 25$,50, and 75 μm, where $r = 100$ μm.

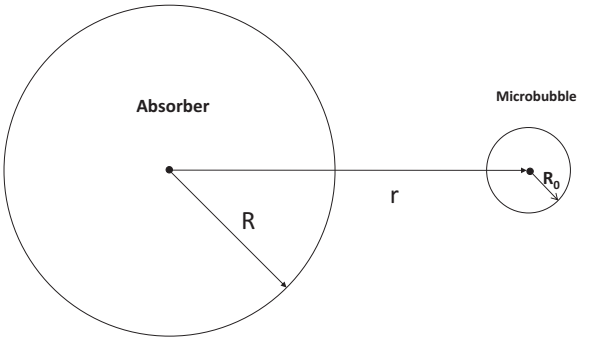

FIG. 3. The absorber and the microbubble with radii of R and R_0, respectively.

and Crum [39] studied the primary radiation force acting on the microbubbles treated as compressible microspheres.

The time average of the product of the fluctuation in the volume of a spherical compressible bubble and the gradient in the acoustic pressure waves creates a radiation force on the bubble given by [33,34]

$$F_{\text{primary}} = \langle V \nabla p(r,t) \rangle , \tag{55}$$

where V and ∇ represent volume of the bubble and gradient in space, respectively. The radiation force is mainly guided by the primary radiation force; the secondary radiation force is negligible with respect to the primary force. In this respect, whenever radiation force is stated it is referred to primary radiation force. The force with the resonant frequency of the microbubble can be simplified to the expression [34]

$$F = \frac{2\pi P_A^2 \tau R_0 \nu_{\text{PRF}}}{\delta_{\text{tot}} \rho v_s \omega_0}, \tag{56}$$

where P_A, τ, R_0, ν_{PRF}, δ_{tot}, ρ, v, and ω_0 stand for the pressure amplitude, pulse duration, radius of the bubble, pulse repetition frequency, total damping constant, density of surrounding medium, speed of sound, and resonant frequency, respectively.

We calculate the radiation force on the microbubble due to the excitation of the absorber illustrated in Fig. 3. When the pulsed laser is sent to the absorber, a photoacoustic wave is generated, leading to a force on the microbubble. We combine the photoacoustic wave expression, which is derived in the previous section, with Leighton's [33] and Dayton *et al.*'s [34] acoustic radiation model to obtain the photoacoustic radiation force.

It is crucial that Eq. (56) is valid only if the resonant frequency of the bubble and the center frequency of the acoustic wave are the same. In addition, the derivation of

TABLE I. Resonant frequency ω_0 and corresponding pulse duration $\tau = \frac{1}{2\omega_0}$ for the microbubbles with diameter of 5 μm [53].

Microbubble	Resonant frequency ω_0 (MHz)	Pulse duration $\tau = \frac{1}{2\omega_0}$(ns)
Sovonue	2.2	227.3
Albunex	5.2	96.1
Quantison	11.0	45.4

TABLE II. Resonant frequency ω_0 and corresponding pulse duration $\tau = \frac{1}{2\omega_0}$ for the microbubbles with a diameter of 10 μm [53].

Microbubble	Resonant frequency ω_0 (MHz)	Pulse duration $\tau = \frac{1}{2\omega_0}$ (ns)
Sovonue	0.9	555.5
Albunex	1.9	263.1
Quantison	4.0	125.0

Eq. (56) is based on a narrowband acoustic excitation [33,34], whereas the photoacoustic wave is usually broadband. However, if the pulse duration of the photoacoustic wave is long, the photoacoustic wave is narrowband [44]. Therefore, our approximation is valid (i) when the center frequency of the photoacoustic wave is very close to the resonant frequency of the microbubble and (ii) when the pulse duration is long. For this reason, in our calculations, the pulse duration is taken such that the center frequency of the photoacoustic wave is equal to the resonant frequency. In other words, the pulse duration is $\tau = \frac{1}{2\omega_0}$. In addition, the pulse duration is also sufficiently long, varying between 45.4 and 555.5 ns, corresponding to the resonant frequencies of the microbubbles given in Tables I and II.

In order to find the force on a microbubble due to the photoacoustic absorber, we first obtain the pressure amplitude of the photoacoustic wave expressed by Eq. (54) in the previous section. Next we calculate the primary radiation force on the microbubble.

Microbubbles vary in their sizes and properties, three of the commercially produced microbubbles—Sovonue, Albunex, and Quantison—are chosen for calculations [53].

The radiation force on each microbubble with respect to the radial distance is investigated. The effect of the beamwidth and pulse repetition frequency on the radiation force is also examined.

For near infrared (970 nm) and visible (596 and 578 nm) wavelengths, the absorption coefficients of whole blood are taken as $\mu_a = 6.9$, 44.8, and 268 cm^{-1}, respectively [54,55]. Parameters of the absorber are $\Gamma = 0.2$, $\eta_{\text{th}} = 1$ [24], and $F = 15$ mJ/cm^2 [56]. The density and the speed of sound are $\rho = 1000$ kg/m^3 and v_s=1480 m/s, respectively [24,34]. Acoustic pulse repetition rates are on the order of kHz. In our case, instead of an acoustic wave generator, the pulsed laser is used to create an acoustic wave by means of the photoacoustic effect. Thus, repetition rates up to the order of MHz are utilized in order to adjust (increase) the radiation force.

In our calculations, the total damping constant for all microbubbles is $\delta_{\text{tot}} = 0.15$ since each diameter is either 5 or 10 μm [53]. Figure 4(a) shows the change of the radiation force on the microbubbles with a diameter of 5 μm, which results from the absorber of radius 75 μm, with respect to the position of the bubbles. The resonant frequencies of aforementioned microbubbles are 2.2, 5.2, and 11 MHz [53], as summarized in Table I. Figure 4(b) shows the change of the force on the bubbles with a diameter of 10 μm and resonant frequencies of 0.9, 1.9, and 4 MHz [53], as summarized in Table II. In Fig. 4, the absorption coefficient of whole blood μ_a is 6.9 cm^{-1}. Figures 5 and 6, recurrently, illustrate the change of the force on the microbubbles with respect to the position of the bubbles for the same parameters except for the absorption coefficients of the whole blood that are $\mu_a = 44.8$, and 268 cm^{-1} for wavelengths of 596 and 578 nm, respectively [54,55]. Here the pulse repetition frequency and the beamwidth are $\nu_{\text{PRF}} = 1$ MHz and $\sigma = 70$ μm, respectively.

In Fig. 7, the effect of the beamwidth on the radiation force is investigated at $r = 75\mu$m for the pulse repetition frequencies, $\nu_{\text{PRF}} = 250$ kHz, 500 kHz, and 1 MHz, respectively, for a microbubble with a diameter of 5 μm. The pulse duration of the laser is 45.4 ns corresponding (or matching) to the resonant frequency of the microbubble which is 11 MHz.

IV. DISCUSSION

In this paper, we first obtain an elaborate expression of the photoacoustic wave and then calculate the corresponding primary radiation force on a microbubble.

First, we solve the photoacoustic wave equation for various spatial and temporal profiles. The selection of these profiles is

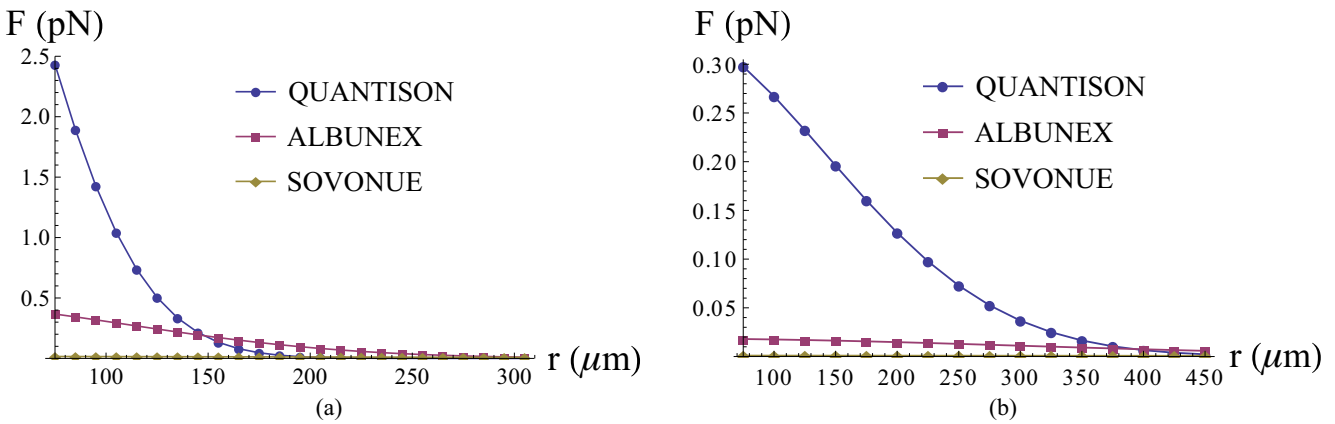

FIG. 4. (Color online) Primary radiation force F (in units of piconewtons) on Sovonue, Albunex, and Quantison vs position r (in units of micrometers) for the diameters of the microbubbles (a) 5 μm with the resonant frequencies of $\omega_0 = 2.2$, 5.2, and 11.0 MHz, respectively, and (b) 10 μm with the resonant frequencies of $\omega_0 = 0.9$, 1.9, and 4.0 MHz, respectively, where the pulse duration $\tau = \frac{1}{2\omega_0}$, the absorption coefficient of whole blood $\mu_a = 6.9$ cm^{-1}, pulse repetition frequency $\nu_{\text{PRF}} = 1$ MHz, and beamwidth $\sigma = 70$ μm.

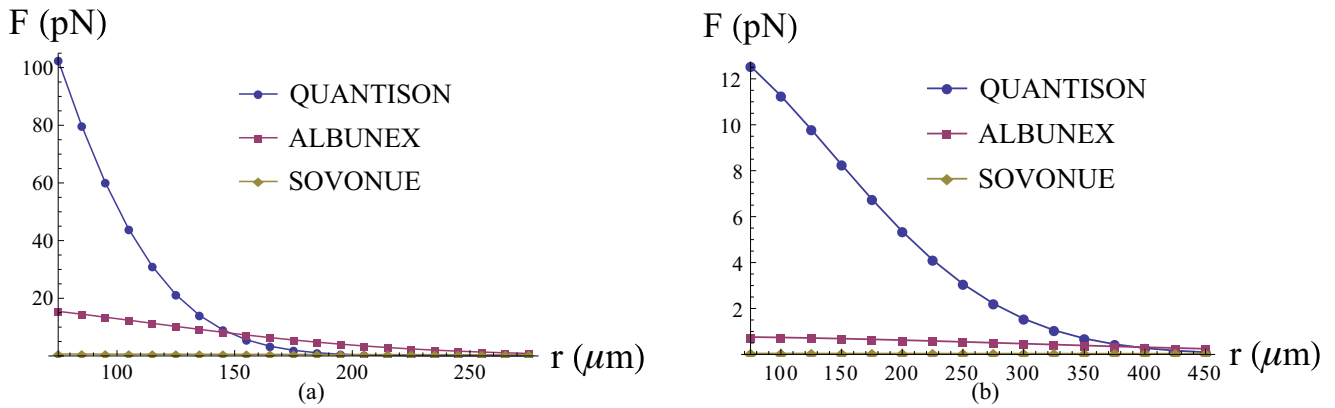

FIG. 5. (Color online) Primary radiation force F (in units of piconewtons) on Sovonue, Albunex, and Quantison vs position r (in units of micrometers) for the diameters of the microbubbles (a) 5 μm with the resonant frequencies of $\omega_0 = 2.2$, 5.2, and 11.0 MHz, respectively, and (b) 10 μm with the resonant frequencies of $\omega_0 = 0.9$, 1.9, and 4.0 MHz, respectively, where the pulse duration $\tau = \frac{1}{2\omega_0}$, the absorption coefficient of whole blood $\mu_a = 44.8\ \text{cm}^{-1}$, pulse repetition frequency $\nu_{\text{PRF}} = 1$ MHz, and beam width $\sigma = 70$ μm.

important since it determines both the magnitude and the form of the photoacoustic wave [2,25,27,30,31,49]. For example, in the literature the temporal profile is usually approximated by a Dirac δ function since the pulse duration is usually very short. However, in our work, the temporal profile is taken as Gaussian that leads to a wave expression including explicit laser parameters, the pulse duration, and the beamwidth. Hence, our approach to find a photoacoustic wave can also be used for the slow heat deposition as well as for the fast heat deposition depending on the pulse duration [49,57]. In addition, we also approximate the absorption profile by a Gaussian function under the assumption that the heat deposition is localized. Note that if the heat deposition is uniform, the absorption profile can be taken as rectangular. As a result, we obtain a photoacoustic wave that is explicitly dependent on the pulsed laser parameters. This allows us to investigate the photoacoustic signal as a function of beamwidth, pulse duration, and repetition rate.

We show the effect of the laser beamwidth on the photoacoustic signal in Fig. 1. In that figure, the change of the normalized photoacoustic wave is given as a function of the normalized time for various beamwidth values. It is seen that the form of the wave approaches an N shape as the beamwidth of the laser pulse becomes comparable to the radius of the object which also provides an explicit laser parameter dependence. Moreover, if the radius of the object is much greater than the beamwidth of the laser, the Gaussian spatial profile behaves like a δ function. This can also be observed in Fig. 1 where the amplitude diminishes as the beamwidth decreases.

We also show the impact of pulse duration on the wave for various beamwidth. It is already well known that the amplitude of the photoacoustic wave decreases as the pulse duration gets longer. The peak power is hence inversely proportional to the pulse duration if the pulse energy of the laser is constant. Therefore, shorter pulse durations yield larger wave amplitudes accompanied by a deterioration in depth resolution. In Fig. 2, as the beamwidth decreases, the signal decreases slightly because the radial profile becomes very sharp approaching a δ function. Therefore, the explicit

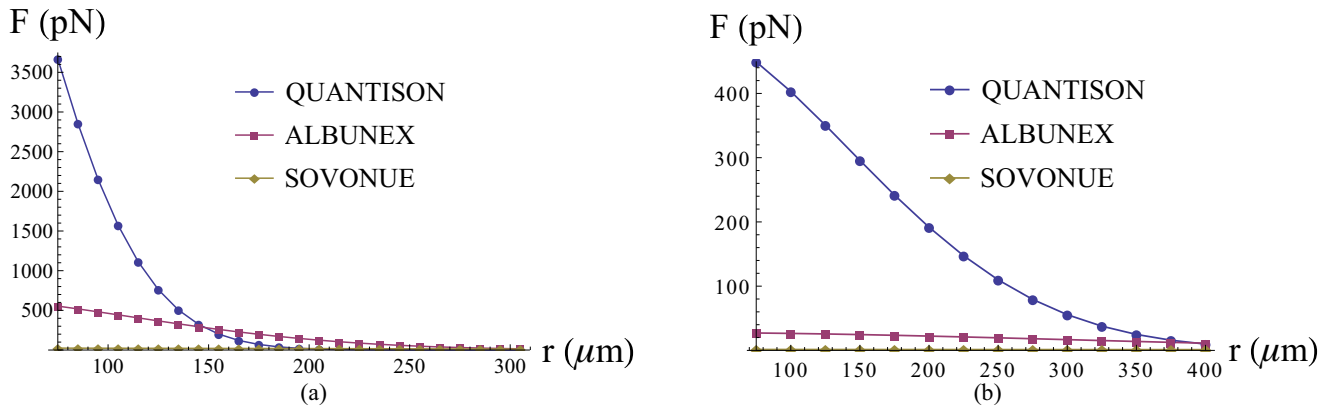

FIG. 6. (Color online) Primary radiation force F (in units of piconewtons) on Sovonue, Albunex, and Quantison vs position r (in units of micrometers) for the diameters of the microbubbles (a) 5 μm with the resonant frequencies of $\omega_0 = 2.2$, 5.2, and 11.0 MHz, respectively, and (b) 10 μm with the resonant frequencies of $\omega_0 = 0.9$, 1.9, and 4.0 MHz, respectively, where the pulse duration $\tau = \frac{1}{2\omega_0}$, the absorption coefficient of whole blood $\mu_a = 268\ \text{cm}^{-1}$, pulse repetition frequency $\nu_{\text{PRF}} = 1$ MHz, and beam width $\sigma = 70$ μm.

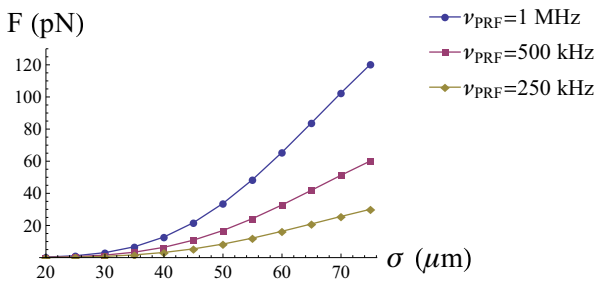

FIG. 7. (Color online) Primary radiation force F (in units of piconewtons) on Quantison vs beamwidth σ (in units of micrometers) for the pulse repetition frequencies of $\nu_{\mathrm{PRF}} = 250$ kHz, 500 kHz, and 1 MHz, respectively, at $r = 75$ μm, where $\omega_0 = 11$ MHz, the pulse duration $\tau = \frac{1}{2\omega_0}$, the absorption coefficient of whole blood is $\mu_a = 44.8$ cm^{-1}, and the diameter of the microbubble 5 μm.

laser parameter dependence disappears. For a very large pulse duration, the wave diminishes since the stress and thermal confinement conditions are violated.

In the second part of the paper, we calculate the photoacoustic radiation force on a microbubble. We achieve this by utilizing the photoacoustic wave expression obtained in Sec. II with the primary radiation force [33,34]. We express the force in terms of the laser parameters. It is important that this expression is valid only if the center frequency of the photoacoustic wave is very close to the resonant frequency of the bubble. The pulse duration is chosen such that the correspondent center frequency of the wave is equal to the resonant frequency of the microbubble. The broadband nature of a photoacoustic wave may also lead to an overestimation of the applied force. However, if the pulse duration is long enough, then the photoacoustic wave is narrowband [44]. For this reason, our results are based relatively on the long pulse duration.

Our calculations show that the force on the microbubble is decreasing with the distance, as expected. Figures 4–6 state that the higher frequency leads to the higher force. According to Eq. (56), the force is inversely proportional to the resonant frequency. However, adjusting the pulse duration according to the resonant frequency leads to a higher amplitude and force in Eq. (56).

A comparison among Figs. 4–6 indicates that the absorption coefficient has a considerable effect on the force. Especially for the absorption coefficient of whole blood corresponding to a visible wavelength of around 578 nm [54,55], the force increases dramatically. In addition, the absorption coefficient can also be increased by using contrast agents. For example, the optical absorption coefficient of whole blood for a wavelength of 800 nm, is around 4–5 cm^{-1}, 16 cm^{-1} for Indocyanine Green (ICG) in water, and 43 cm^{-1} for ICG in blood [58,59]. Richness of optical contrast agents is another advantage for manipulation of microbubbles with photoacoustic radiation force. On the other hand, it should be noted that when the absorption coefficient increases, penetration depth in tissue decreases. There is a compromise between the increase in force and penetration depth via absorption coefficient adjustment. Figures 5 and 6 indicate that the force can reach the order of 100 and 1000 pN using the visible wavelengths. Application of the force at this scale makes the manipulation and confinement of the microbubbles possible to enhance the image quality and drug delivery. At least forces of a few hundred piconewtons are needed to manipulate the microbubbles in biological applications [45]. In addition, considerably small forces ($<$10 pN) can be used to measure viscoelastic properties of the microbubbles [46]. As the microbubble is farther away from the absorber, the force decreases as expected. Our results are in good agreement with Zharov's and Hernot's experimental results [40,43].

The radiation force increases with the beamwidth, as can be seen in Fig. 7. The reason for this increase is that the laser pulse with a large beamwidth is absorbed by the larger part of the absorber. In Fig. 7, the force is shown to be increasing with the pulse repetition frequency.

Therefore, a comprehensive understanding of the primary radiation force and analytical solutions to the photoacoustic wave equation make adjustment of parameters specifically for biological applications possible.

ACKNOWLEDGMENTS

We would like to thank all the reviewers for their instructive and valuable comments. This research is supported in part by Marie Curie Reintegration Grant No. 268287, Bogazici University Research funding Grant No. BAP 7126 and TUBITAK Grant No. 112T253.

[1] A. A. Karabutov, N. B. Podymova, and V. S. Letokhov, Appl. Opt. **34**, 1484 (1995).
[2] C. G. A. Hoelen, F. F. M. de Mul, R. Pongers, and A. Dekker, Opt. Lett. **23**, 648 (1998).
[3] R. A. Kruger, K. K. Kopecky, A. M. Aisen, D. R. Reinecke, G. A. Kruger, and W. L. Kiser, Radiology **211**, 275 (1999).
[4] L. V. Wang, X. Zhao, H. Sun, and G. Ku, Rev. Sci. Instrum. **70**, 3744 (1999).
[5] G. Ku and L. V. Wang, Med. Phys. **27**, 1195 (2000).
[6] M. Xu, G. Ku, and L. V. Wang, Med. Phys. **28**, 1958 (2001).
[7] Y. Xu and L. V. Wang, Med. Phys. **28**, 1519 (2001).
[8] M. Xu and L. V. Wang, IEEE Trans. Med. Imaging **21**, 814 (2002).
[9] R. O. Esenaliev, I. V. Larina, K. V. Larin, D. J. Deyo, M. Motamedi, and D. S. Prough, Appl. Opt. **41**, 4722 (2002).
[10] Y. Xu, D. Feng, and L. V. Wang, IEEE Trans. Med. Imaging **21**, 823 (2002).
[11] Y. Xu and L. V. Wang, Phys. Rev. Lett. **92**, 033902 (2004).
[12] L. V. Wang, IEEE J. Sel. Top. Quantum Electron. **14**, 171 (2008).
[13] W. Shi, P. Hajireza, P. Shao, A. Forbrich, and J. Z. Roger, Opt. Express **19**, 17143 (2011).

[14] Z. Xie, S. L. Chen, T. Ling, L. J. Guo, P. L. Carson, and X. Wang, Opt. Express **19**, 9027 (2011).
[15] J. Zhang, M. A. Anastasio, P. J. Rivière, and L. H. V. Wang, IEEE Trans. Med. Imaging **28**, 1781 (2009).
[16] D. Hutchins and A. C. Tam, IEEE Trans. Ultrason. Ferroelectr. Freq. Control **33**, 427 (1986).
[17] A. C. Tam, Rev. Mod. Phys. **58**, 381 (1986).
[18] J. Ripoll and V. Ntziachristos, Phys. Rev. E **71**, 031912 (2005).
[19] P. Beard, Interface Focus **1**, 602 (2011).
[20] S. Hu, K. Maslov, and L. H. V. Wang, Opt. Express **17**, 7688 (2009).
[21] J. Gamelin, A. Maurudis, A. Aguirre, F. Huang, P. Guo, L. H. V. Wang, and Q. Zhu, Opt. Express **17**, 10489 (2009).
[22] L. V. Wang, Dis. Markers **19**, 123 (2004).
[23] M. Xu and L. V. Wang, Rev. Sci. Instrum. **77**, 041101 (2006).
[24] L. H. V. Wang and H. Wu, *Biomedical Optics: Principles and Imaging* (Wiley, New Jersey, 2007).
[25] M. W. Sigrist and F. K. Kneubühl, J. Acoust. Soc. Am. **64**, 1652 (1978).
[26] H. M. Lai and K. Young, J. Acoust. Soc. Am. **72**, 2000 (1982).
[27] G. J. Diebold, T. Sun, and M. I. Khan, Phys. Rev. Lett. **67**, 3384 (1991).
[28] V. N. Inkov, A. A. Karabutov, and I. M. Pelivanov, Laser Phys. **11**, 1283 (2001).
[29] V. Kozhushko, T. Khokhlova, A. Zharinov, I. Pelivanov, V. Solomatin, and A. Karabutov, J. Acoust. Soc. Am. **116**, 1498 (2004).
[30] G. J. Diebold and J. Westervelt, J. Acoust. Soc. Am. **84**, 2245 (1988).
[31] I. G. Calasso, W. Craig, and G. J. Diebold, Phys. Rev. Lett. **86**, 3550 (2001).
[32] M. A. Anastasio, J. Zhang, D. Modgil, and P. J. La Rivière, Inverse Probl. **23**, S21 (2007).
[33] T. G. Leighton, *The Acoustic Bubble* (Academic Press, San Diego, CA, 1994).
[34] P. A. Dayton, K. E. Morgan, A. L. S. Klibanov, G. Brandenburger, K. R. Nightingale, and K. W. Ferrara, IEEE Trans. Ultrason. Ferroelectr. Freq. Control **44**, 1264 (1997).
[35] X. Zheng and R. Apfel, J. Acoust. Soc. Am. **97**, 2218 (1995).
[36] C. P. Lee and T. G. Wang, J. Acoust. Soc. Am. **93**, 1637 (1993).
[37] R. Lofstedt and S. Putterman, J. Acoust. Soc. Am. **90**, 2027 (1991).
[38] J. Wu and G. Du, J. Acoust. Soc. Am. **87**, 997 (1990).
[39] L. Crum, J. Acoust. Soc. Am. **57**, 1363 (1975).
[40] S. Hernot and A. L. Klibanov, Adv. Drug Delivery Rev. **60**, 1153 (2008).
[41] A. F. H. Lum, M. A. Borden, P. A. Dayton, D. E. Kruse, S. I. Simon, and K. W. Ferrara, J. Controlled Release **111**, 128 (2006).
[42] P. H. Jones, E. Stride, and N. Saffari, Appl. Phys. Lett. **89**, 081113 (2006).
[43] V. P. Zharov, T. V. Malinsky, and R. C. Kurten, J. Phys. D: Appl. Phys. **38**, 2662 (2005).
[44] N. Wua, Y. Tiana, X. Zoub, and X. Wang, Proc. SPIE **8694**, 869401 (2013).
[45] A. L. Klibanov, M. S. Hughes, F. S. Villanueva, R. J. Jankowski, W. R. Wagner, J. K. Wojdyla, J. H. Wible, and G. H. Brandenburger, Magma Magn. Reson. Mater. Phys. Biol. Med. **8**, 177 (1999).
[46] V. Sboros, Adv. Drug Delivery Rev. **60**, 1117 (2008).
[47] P. M. Morse and H. Feshbach, *Methods of Theoretical Physics, Part I* (McGraw-Hill, New York, 1953).
[48] C. G. A. Hoelen and F. F. M. de Mul, J. Acoust. Soc. Am. **106**, 695 (1999).
[49] G. J. Diebold, A. C. Beveridge, and T. J. Hamilton, J. Acoust. Soc. Am. **112**, 1780 (2002).
[50] Y. N. Cao, H. X. Chen, T. Sun, G. J. Diebold, and M. B. Zimmt, J. Phys. IV **04**, C7-713 (1994).
[51] X. Wang, Y. Pang, G. Ku, X. Xie, G. Stoica, and L. H. V. Wang, Nat. Biotech. **21**, 803 (2003).
[52] Y. Wang, X. Xie, X. Wang, G. Ku, K. L. Gill, D. P. O'Neal, G. Stoica, and L. H. V. Wang, Nano Lett. **4**, 1689 (2004).
[53] N. de Jong, A. Bouakaz, and P. Frinking, Echocardiography **19**, 229 (2002).
[54] H. F. Zhang, K. Maslov, G. Stoica, and L. V. Wang, Nat. Biotechnol. **24**, 848 (2006).
[55] N. Bosschaart, G. J. Edelman, M. C. G. Aalders, T. G. van Leeuwen, and D. J. Faber, Lasers Med. Sci. **29**, 453 (2014).
[56] S. J. Yoon, A. Murthy, K. P. Johnston, K. V. Sokolov, and S. Y. Emelianov, Opt. Express **20**, 29479 (2012).
[57] S. M. Park, M. I. Khan, H. Z. Cheng, and G. J. Diebold, Ultrasonics **29**, 63 (1991).
[58] G. Ku and L. V. Wang, Opt. Lett. **30**, 507 (2005).
[59] M. L. Landsman, G. Kwant, G. A. Mook, and W. G. Zijlstra, J. Appl. Physiol. **40**, 575 (1976).